VOLUME 79 SEPARATE No. 182

PROCEEDINGS

AMERICAN SOCIETY
OF
CIVIL ENGINEERS

APRIL, 1953

HIPPED PLATE ANALYSIS, CONSIDERING JOINT DISPLACEMENTS

By Ibrahim Gaafar, A.M. ASCE

STRUCTURAL DIVISION

Headquarters of the Society
33 W. 39th St.
New York 18, N.Y.

PRICE $0.50 PER COPY

GUIDEPOST FOR TECHNICAL READERS

"Proceedings-Separates" of value or significance to readers in various fields are here listed, for convenience, in terms of the Society's Technical Divisions. Where there seems to be an overlapping of interest between Divisions, the same Separate number may appear under more than one item. For a description of papers open to discussion refer to the current issue of *Civil Engineering*.

Technical Division	*Proceedings-Separate Number*
Air Transport	108, 121, 130, 148, 163, 172, 173, 174, 181, 187 (Discussion: D-75, D-93, D-101, D-102, D-103, D-108, D-121)
City Planning	151, 152, 154, 164, 167, 171, 172, 174, 177 (Discussion: D-65, D-86, D-93, D-99, D-101, D-105, D-108, D-115, D-117)
Construction	160, 161, 162, 164, 165, 166, 167, 168, 181, 183, 184, (Discussion: D-75, D-92, D-101, D-102, D-109, D-113, D-115, D-121, D-126, D-128, D-136)
Engineering Mechanics	145, 157, 158, 160, 161, 162, 169, 177, 179, 183, 185, 186, (Discussion: D-24, D-33, D-34, D-49, D-54, D-61, D-96, D-100, D-122, D-125, D-126, D-127, D-128, D-135, D-136)
Highway	144, 147, 148, 150, 152, 155, 163, 164, 166, 168, 185 (Discussion: D-103, D-105, D-108, D-109, D-113, D-115, D-117, D-121, D-123, D-128)
Hydraulics	154, 159, 164, 169, 175, 178, 180, 181, 184, 186, 187 (Discussion: D-90, D-91, D-92, D-96, D-102, D-113, D-115, D-122, D-123, D-135)
Irrigation and Drainage	148, 153, 154, 156, 159, 160, 161, 162, 164, 169, 175, 178, 180, 184, 186, 187 (Discussion: D-102, D-109, D-117, D-135)
Power	130, 133, 134, 135, 139, 141, 142, 143, 146, 148, 153, 154, 159, 160, 161, 162, 164, 169, 175, 178, 180, 184, 186 (Discussion: D-96, D-102, D-109, D-112, D-117, D-135)
Sanitary Engineering	55, 56, 87, 91, 96, 106, 111, 118, 130, 133, 134, 135, 139, 141, 149, 153, 166, 167, 175, 176, 180, 187 (Discussion: D-97, D-99, D-102, D-112, D-117, D-135)
Soil Mechanics and Foundations	43, 44, 48, 94, 102, 103, 106, 108, 109, 115, 130, 152, 155, 157, 166, 177 (Discussion: D-86, D-103, D-108, D-109, D-115)
Structural	145, 146, 147, 150, 155, 157, 158, 160, 161, 162, 163, 164, 165, 166, 168, 170, 175, 177, 179, 181, 182, 183, 185, 188 (Discussion: D-51, D-53, D-54, D-59, D-61, D-66, D-72, D-77, D-100, D-101, D-103, D-109, D-121, D-125 D-126, D-127, D-128, D-136)
Surveying and Mapping	50, 52, 55, 60, 63, 65, 68, 121, 138, 151, 152, 172, 173 (Discussion: D-60, D-65)
Waterways	123, 130, 135, 148, 154, 159, 165, 166, 167, 169, 181 (Discussion: D-19, D-27, D-28, D-56, D-70, D-71, D-78, D-79, D-80, D-112, D-113, D-115, D-123, D-135)

A constant effort is made to supply technical material to Society members, over the entire range of possible interest. Insofar as your specialty may be covered inadequately in the foregoing list, this fact is a gage of the need for your help toward improvement. Those who are planning papers for submission to "Proceedings-Separates" will expedite Division and Committee action measurably by first studying the ASCE "Guide for Development of Proceedings-Separates" as to style, content, and format. For a copy of this pamphlet, address the Manager, Technical Publications, ASCE, 33 W. 39th Street, New York 18, N. Y.

Published at Prince and Lemon Streets, Lancaster, Pa., by the American Society of Civil Engineers. Editorial and General Offices at 33 West Thirty-ninth Street, New York 18, N. Y.

Proceedings—Vol. 79 April, 1953 Separate No. 182

AMERICAN SOCIETY OF CIVIL ENGINEERS

Founded November 5, 1852

PAPERS

HIPPED PLATE ANALYSIS, CONSIDERING JOINT DISPLACEMENTS

By Ibrahim Gaafar,[1] A. M. ASCE

Synopsis

Both theoretical and experimental investigations of the structural action of hipped plate structures are presented in this paper. The relative displacements of the joints of such structures under loading, neglected in the approximate theory of design described by G. Ehlers and H. Craemer, are shown to affect the results materially, and are taken into consideration by a more accurate, but still practical, method of analysis.

Tests on a $\frac{1}{40}$-scale aluminium model of a hipped plate roof have justified the assumptions and verified the analytical results. The results obtained by use of the different theories are compared and checked against the experimental results.

The results of the approximate theory of Messrs. Ehlers and Craemer showed an average discrepancy of 200% in the values of the longitudinal stresses, and at some points gave opposite signs to the experimental results. The proposed treatment showed an average discrepancy of 40% for the same case. Referring to the transverse stresses, the approximate theory errs greatly (from + 60% to − 280%) on the unsafe side, and the proposed theory errs by 20% on the safe side.

The analytical values of the displacements of the joints yielded by the proposed theory agreed well with the experimental values. The difference between both results ranged from 2% for large displacements to 25% for small displacements.

Note.—Written comments are invited for publication; the last discussion should be submitted by October 1, 1953.

[1] Assist. Prof. of Structural Eng., Ibrahim Univ., Cairo, Egypt.

INTRODUCTION

Notation.—The letter symbols in this paper are defined where they first appear, in the text or by diagram, and are assembled alphabetically in the Appendix.

No particular sign convention was found necessary for the displacements, the forces, or the stresses. Any assumed displacements may be considered positive. A negative value in the result means an opposite sense of displacement to the one first assumed. Consistency in working out the solution, rather than a specified sign convention, is essential. For the sake of brevity as suggested by G. Winter, M. ASCE, and M. Pei,[2] J. M. ASCE, bending of a plate out of its plane will be designated as slab action and bending in its plane, plate action.

Previous Theory.—The principle of hipped plate construction was first developed by G. Ehlers in Germany in 1924. He wrote the first technical paper[3] on this subject in 1930. In his method of analysis he considered the different plate elements as beams supported at the cross and end diaphragms, shown in Fig. 1. Along the longitudinal edges, the plates were assumed to be

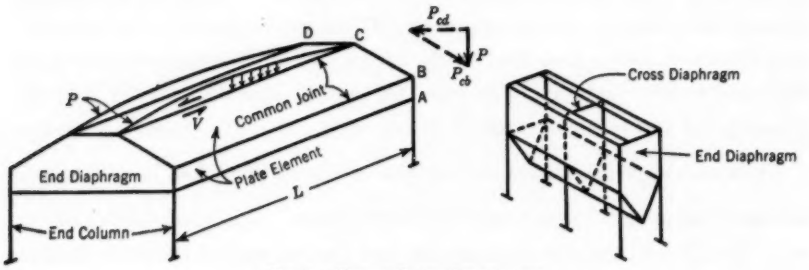

FIG. 1.—HIPPED PLATE STRUCTURES

connected by hinged joints that do not slide longitudinally and that are considered capable of transferring only edge shears, V, between the contiguous plate elements. Such connections neglected entirely the connecting moments transmitted between the plates due to the rigidity of the joints. The uniform loads on the plates were transformed to the line loads P acting at the joints. These loads P were resolved into two components P_{cd} and P_{cb} parallel to the two adjacent plates as shown in Fig. 1. The plates, acting as beams between the diaphragms, carried the loads P. At the same time, the shear stresses V were created to maintain equal longitudinal strains along the common edges. This strain condition at each joint was used to determine the magnitude and distribution of the edge shear stresses V.

In 1932, E. Gruber published a paper[4] in which he considered the effect of the rigidity of the joints, the connecting moments acting along the common

[2] "Hipped Plate Construction," by G. Winter and M. Pei, *Journal*, A. C. I., January, 1947.

[3] "Ein neues Konstruktionprinzip, " by G. Ehlers, *Bauingenieur*, Vol. 9, 1930, p. 125.

[4] "Berechnung Prismatischer Scheibenwerke," by E. Gruber, *Memoirs*, International Assn. of Bridge and Structural Eng., Vol. 1, 1932, p. 225.

edges of the plates, and the effect of the relative dsiplacements between the joints. As a first approximation, the hipped roof was assumed to be hinged along the joints. By using this assumed hinged structure as a basic system, he developed his solution in the form of simultaneous differential equations of the fourth order, which could be solved by rapidly converging series. For a hipped roof of $r + 1$ plates, r being the number of joints, the total number of unknowns is $7\,r + 2$. For a roof of five plates, this will involve thirty unknowns. The solution is complicated even if trigonometric series are used. In his solution, Mr. Gruber showed that the maximum longitudinal stresses on a cross section and the maximum deflections for a roof with hinged plates were about twice as great as those for the rigidly connected plates. Consequently, he concluded that the influence of the rigid connections ought not to be neglected as it had been according to the usual practice.

Later, the theory was further developed and expanded in many respects by H. Craemer,[5,6] Mr. Gruber,[7] and others. The European literature on the subject, mostly in German, is fairly extensive. All the treatments of the theory by German authors are developed from elasticity equations in the form of simultaneous algebraic and differential equations mathematically involved. With the exception of Mr. Gruber,[4] all writers have made the same simplifying assumption of neglecting the effect of the relative deflections of the joints—including Messrs. Craemer[5,6,8] and Ehlers[3] who first established the current simplified theory, taking into consideration the rigidity of the joints and the resulting transverse connecting moments.

In January, 1947, Messrs. Winter and Pei of Cornell University at Ithaca, N. Y., published a paper[2] on hipped plate construction in which they transformed the algebraic solution into a stress distribution method, which has the advantage of numerical simplicity over the other procedures. However, they also made the same simplifying assumption of neglecting the effect of the relative deflections of the joints.

In a dissertation[9] submitted to Cornell University in 1948, Mr. Pei presented a method of analysis considering joint displacements. The method requires the solution of $6\,n + 1$ simultaneous algebraic equations in which n is the number of plates. For a roof of five plates as shown in Fig. 1, the number of equations is thirty one.

None of the mathematical investigations previously mentioned gives any experimental evidence to substantiate the assumptions and verify the analytical procedures that were used. It seems that no previous experimental evidence from either actual structures or small-scale models has been obtained to support the theoretical analysis.

In the development of the analysis proposed in this paper, it was found necessary to depend on a study of the deformations and joint displacements in small-scale models to check and support the proposed theoretical analysis.

---

[5] "Der Heutige Stand der Theorie der Scheibentraeger und Faltwerke, in Eisenbeton," by H. Craemer, *Beton und Eisen*, Vol. 36, 1937, p. 264.

[6] *Ibid.*, p. 297.

[7] "Die Berechnung pyramidenartiger Scheibenwerke und ihre Anwendung auf Kaminkeuhler," by E. Gruber, *Memoirs*, International Assn. of Bridge and Structural Eng., Vol. 2, 1933–1934, p. 206.

[8] "Theorie der Faltwerke," by H. Craemer, *Beton und Eisen*, Vol. 29, 1930, p. 276.

[9] "Hipped Plate Structures," by M. Pei, thesis presented to Cornell University, at Ithaca, N. Y., 1948, in partial fulfilment of the requirements for the degree of Doctor of Philosophy.

Limitations

The limitations governing Mr. Gruber's solution[4] will also be used in the theoretical investigation. They are as follows: (1) All plates are of rectangular shape. (2) The length of each plate is more than twice its width. This limitation makes it possible to treat the plates as one-way slabs, to assume linear distribution of bending stresses, and to neglect the effect of torsional rigidity. This treatment is justified by the experimental results obtained (see Fig. 28, appearing subsequently). (3) The structure is monolithically built. All joints are rigid. (4) Each plate is of uniform thickness. (5) The material is homogeneous and elastic. The theoretical and experimental investigations given herein are readily applicable to hipped plate structures built of steel or any elastic material. As for application to reinforced concrete, this paper provides some light on the subject, and it is recommended that further experimental and analytical studies be made of reinforced concrete models. (6) In any plate, plane sections remain plane after deformation. The measured longitudinal strains shown in Figs. 23 and 24, appearing subsequently, are fairly linear across each plate and seem to justify this assumption. Plane cross sections of the entire structure do not necessarily remain plane after deformation.

Relative Transverse Displacements Between Joints

In the method of analysis proposed in this paper, the relative transverse displacement Δ, between any two consecutive joints, is chosen as an unknown, and is treated as an additional load on the roof. These displacements will affect the slab moments, shears, and, consequently, the plate loads, P, and the plate deflections, δ. For a loading that is symmetrical about the middle section of the roof, the relative displacements are maximum at the middle of the span and are zero at the end diaphragms. If the maximum relative displacements between two joints are assigned a value Δ_0, three points will be given on the curve for the relative displacement. The general form of the curve is known but its exact equation is not known. The best approximation for such a curve may be the elastic line of a beam loaded in a similar way as is the roof. That is, if the roof is uniformly loaded (which is usually the case), then the Δ-curve may be assumed to follow the elastic line of a uniformly loaded beam.

In the case of single-span roofs symmetrically loaded with respect to the middle of the span, the relaitve Δ-values can be represented by a half wave of a sine curve, instead of assuming them to vary as the elastic line of the corresponding loaded beam. This is shown by studying and comparing the curves represented by Eqs. 1, as follows:

The elastic line of a beam that carries a uniform load, and that has the maximum deflection Δ_0 at the middle, is expressed by

$$\Delta = \Delta_0 \left(\frac{16}{5} \frac{x^4}{L^4} - \frac{24}{5} \frac{x^2}{L^2} + 1 \right) \ldots\ldots\ldots\ldots\ldots\ldots (1a)$$

The equation for the elastic line of a beam loaded with a concentrated load at the middle, and also having the maximum deflection Δ_0 at the middle, is

$$\Delta = \Delta_0 \left(4 \frac{x^3}{L^3} - 6 \frac{x^2}{L^2} + 1 \right) \ldots\ldots\ldots\ldots\ldots\ldots (1b)$$

and that for a half sine wave is

$$\Delta = \Delta_0 \sin \frac{\pi x}{L} \quad \ldots\ldots\ldots\ldots\ldots\ldots\ldots\ldots\ldots\ldots (1c)$$

In the foregoing expressions, x represents distance parallel to the joints, measured from the left end of the structure. These three curves, when plotted, are so nearly alike as to be almost indistinguishable. They have the same maximum ordinate Δ_0, and at the quarter points of the span these curves have their ordinates equal to $\frac{57}{80}\Delta_0$, $\frac{55}{80}\Delta_0$, and $\frac{56.6}{80}\Delta_0$, respectively.

When Eqs. 1 are treated as load curves on the plate elements of the roof, their correcting effects, δ_2, on the plate deflections, δ, at the middle of the span will be still more alike. If the relative deflections are assumed to vary according to Eqs. 1*b* and 1*c*, respectively, then the respective values for δ_2 will be 0.1010 multiplied by a constant (for Eq. 1*b*) and 0.1024 multiplied by the same constant (for Eq. 1*c*). These two values agree well, and, in the case of Eq. 1*a* and the sine curve (Eq. 1*c*), the agreement of results will be still closer.

This agreement suggests the adoption of Eq. 1*c*, the half sine wave, to represent the manner in which the Δ-values vary in single-span roofs. If this procedure is adopted, the loads on the roof may be either uniform or concentrated, provided that they are symmetrical about the middle of the span. Such use of the sine curve greatly simplifies the analytical treatment.

In the case of multispan roofs, or of roofs on which the loads are far from being symmetrical about the middle of the span, this sine wave treatment cannot be used with accuracy, and the elastic line of the corresponding loaded beam would have to be adopted—for the present. However, there may be a way of introducing a simplification, even in such a case.

Proposed Method of Analysis

The proposed method of analysis will be explained in terms of its application to the roof shown in Fig. 2. Of primary concern is the analytical deter-

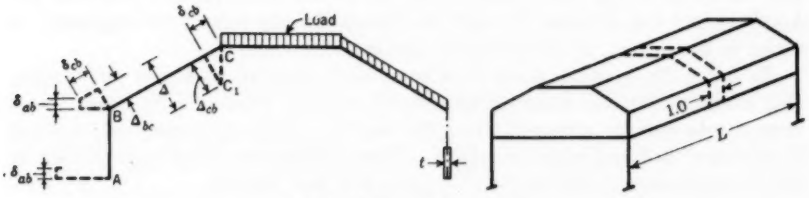

Fig. 2.—A Hipped Plate Roof

mination of the relative transverse displacements (Δ) of the joints and their effect on the magnitude and distribution of the internal transverse and longitudinal stresses in the structure.

1. The first step in the analysis is the computation of the forces and of the transverse and longitudinal stresses acting at the edges of each plate element, neglecting the effect of the relative displacement of the joints. The analytical

procedure used by Messrs. Winter and Pei[2,9] provides a convenient solution for this problem. In this procedure, the roof in the transverse direction is considered as a continuous one-way slab supported on rigid supports at the joints, and thus the shear forces Q are readily obtained. The Q-forces at each joint are then resolved into two component P-forces parallel to the contiguous plates. The plates, acting as beams between the diaphragms, carry the P-loads (plate action). At the same time, edge shear stresses (V) are created along the edges to maintain equal longitudinal strains along the common edges. The longitudinal (plate) stresses at a section of the roof, caused by the P-forces only, are corrected in a manner similar to the moment-distribution method, to include the effect of the edge shear stresses V.

2. The second step in the analysis is to provide for the effect that the relative transverse displacement of the joints has on the transverse and longitudinal stresses. This operation is most easily accomplished by choosing the relative transverse displacements (Δ) between each pair of consecutive joints as unknowns, determining the corresponding transverse (slab) fixed-end moments in terms of the Δ-values, and correcting for rotation at the ends of the slab strips by the moment-distribution method. After the end moments have been determined, the Q-forces and P-forces are computed in the same manner as in step 1. This operation must be repeated for each different Δ-value. For unsymmetrical loading, the number of unknown Δ-values for the structure in Fig. 2 is equal to three, but there is only one unknown for symmetrical loading.

3. After the Q-forces and P-forces have been expressed in terms of the Δ-values, the corresponding longitudinal (plate) stresses are computed in the same manner as in step 1.

4. From the values of the longitudinal stresses yielded in steps 1 and 3, the plate deflections δ_1 and δ_2 are computed. Therefore, the sum, δ, of these plate deflections is in terms of the applied load and the relative transverse deflection Δ. It will be found that there is only one set of Δ-values that will satisfy the algebraic relations between the Δ-values and the δ-values imposed by the geometrical requirements of the cross section and the equilibrium conditions. The values of Δ can be computed from the geometrical relations between the Δ-values and the δ-values because the latter already have been expressed in terms of the former by the computations in steps 2 and 3.

5. After the Δ-values have been computed, the slab moments and shears, and consequently the longitudinal (plate) stresses produced by these transverse displacements, are known because they have been previously (steps 2 and 3) expressed in terms of the Δ-values. These values are added algebraically to the corresponding values in step 1 to give the final results.

The application of the foregoing procedure to a $\frac{1}{40}$-scale aluminium model is illustrated in the following pages.

Examples

Example No. 1.—The dimensions of a $\frac{1}{40}$-scale aluminium model of a hipped plate roof, similar to that shown in Fig. 2, are given in Fig. 3. The model is

loaded with a uniform load distributed entirely upon the top plate CC′, and it is required to determine the maximum transverse and longitudinal stresses, produced by this loading, in the model.

Step 1.—For the case of external loads and nonyielding supports, a transverse strip 1.0 in. wide at the middle of the span is considered, treating it as a continuous slab supported at the joints by nonyielding supports. The moment-distribution factors obtained from the stiffness coefficient, c, and the rigidity coefficient, $k = \frac{E\,I}{h}$, are evaluated for this example in Table 1.

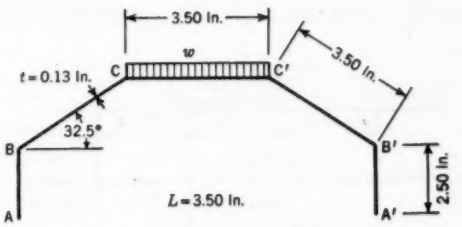

FIG. 3.—ROOF FOR EXAMPLE NO. 1

The fixed-end moment at joint C is equal to $\frac{w\,h^2}{12}$. The bending moments and shears for this case are given in Fig. 4. The Q-forces, that is, the shear forces per unit length, acting on the joints, are given in Fig. 5.

TABLE 1.—MOMENT-DISTRIBUTION FACTORS AT JOINT C

Member	Stiffness coefficient, c	Rigidity coefficient, k, in inch-pounds	$c\,k$	Moment-distribution factor
(1)	(2)	(3)	(4)	(5)
CB	3	1	3	0.60
CC′	2	1	2	0.40
			5	1.00

For the determination of the P-forces acting on the plates, the positive sense for the P-forces may be assumed to be as indicated in Fig. 6. Then—

$$P_{ab} = +\,0.05\,w\,h\,\frac{1}{\cos\theta_b} = +\,0.05\,w\,h\,\frac{1}{0.8434} = +\,0.0593\,w\,h \ldots (2a)$$

$$P_{bc} = -\,0.05\,w\,h\,(\tan\theta_b + \cot\theta_b) - 0.5\,w\,h\,\frac{1}{\sin\theta_b} = -\,1.0424\,w\,h \ldots (2b)$$

and, similarly, the P-force in plate CC′ is zero. In the foregoing computations, $h = 3.5$ in., and the subscripts indicate the joints between which the forces act.

To determine the "free edge" bending moments and the corresponding stresses at the middle section, each plate may be treated as a beam carrying the loads P and spanning between the end diaphragms, with no edge shear V along the joints. The moments, in inch-pounds, are

$$M_{ab} = P_{ab}\frac{L^2}{8} = (+\,0.0593\,w\,h)\,\frac{35.0^2}{8} = +\,31.80\,w \ldots\ldots (2c)$$

$$M_{bc} = P_{bc}\frac{L^2}{8} = (-\,1.0424\,w\,h)\,\frac{35.0^2}{8} = -\,560.0\,w \ldots\ldots (2d)$$

and for plate CC′, the moment is zero.

The corresponding fiber stresses are as follows:

Plate	Section modulus, Z, in cubic inches	Fiber stress, s, in pounds per square inch
AB	0.1354	$\pm 235.0\ w$
BC	0.266	$\pm 2105.0\ w$
CC′	0.266	0.0

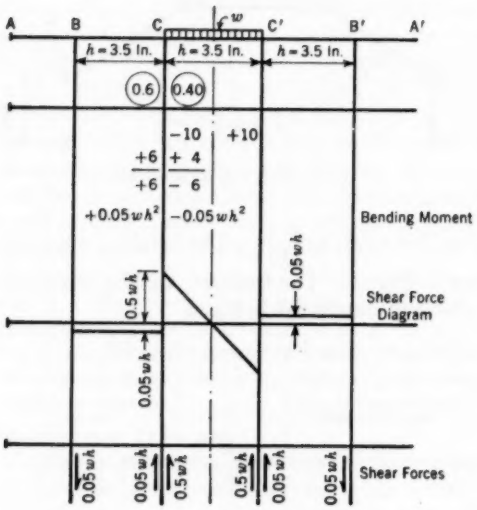

FIG. 4.—MOMENT AND SHEAR VALUES

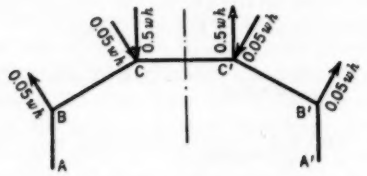

FIG. 5.—LOCATIONS AND DIRECTIONS OF THE Q-FORCES

These free edge stresses are shown in Fig. 7. The signs for the stresses depend on the sense of the corresponding P-loads. The free edge stresses correspond to the case in which longitudinal sliding hypothetically takes place between the adjacent plates. However, this longitudinal sliding is eliminated by the presence of the longitudinal edge shears V between the adjacent edges. To correct the free edge stresses so that they include the effect of edge shear stresses, two equal and opposite forces are introduced, one at each joint. The process is similar to that used in the moment-distribution method.

The stresses in two rectangular sections AB and BC that are acted upon by two equal and opposite edge forces F are shown in Fig. 8. It can be concluded[2] that the stress-distribution coefficients at the joints are as follows:

At joint B,

$$K_{ba} = \frac{\frac{4F}{A_{ba}}}{\frac{4F}{A_{ba}} + \frac{4F}{A_{bc}}} = \frac{A_{bc}}{A_{bc} + A_{ba}} = \frac{3.50}{2.50 + 3.50} = 0.58 \quad \ldots\ldots (3a)$$

Similarly,

$$K_{bc} = \frac{A_{ba}}{A_{ba} + A_{bc}} = 0.42 \quad \ldots\ldots (3b)$$

and at joint C,

$$K_{cb} = -K_{cc'} = 0.50 \quad \ldots\ldots\ldots\ldots\ldots\ldots\ldots\ldots (3c)$$

The carry-over factor equals $-\frac{1}{2}$.

The free edge stresses are corrected in Table 2. They are given in the second line of the table, and the stresses, after distribution, are given in the

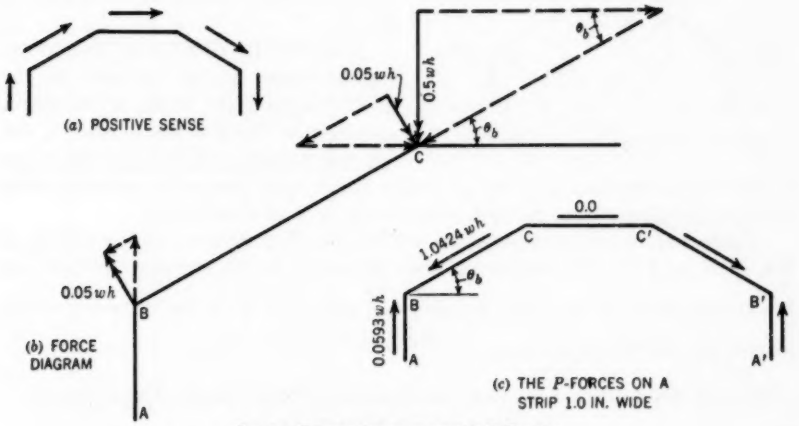

FIG. 6.—DETERMINATION OF THE *P*-FORCES

last line, and are shown on a section of the model Fig. 9. Table 2 shows one half of the symmetrical structure. These stresses represent the longitudinal (plate) stresses at the middle section for the case of external loads, neglecting the effect of the relative displacements of the joints, which will be considered in the next step.

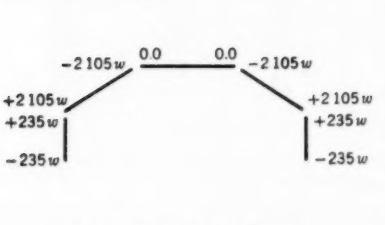

FIG. 7.—FREE EDGE STRESSES

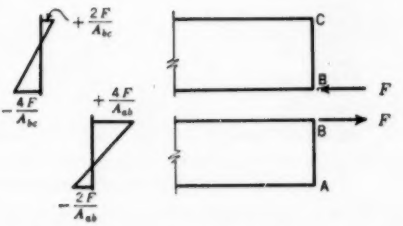

FIG. 8.—STRESSES PRODUCED BY EDGE FORCES

Step 2.—In determining the effect of the relative displacements of the joints, a transverse strip at the middle of the model 1.0 in. wide is considered, and the relative displacement (see Fig. 2) between edges B and C at the middle of the strip is given by $\Delta = \Delta_{bc} + \Delta_{cb}$.

The fixed-end moment at edge C, with edge B free to rotate, equals $3\frac{E\,I}{h}\left(\frac{\Delta}{h}\right) = 3\,\alpha$, in which I equals the moment of inertia of a strip 1.0 in.

wide. For the plate in this example, $I = 183 \times 10^{-6}$ in.^{4}. The symbol E is the modulus of elasticity of aluminium, which is equal to 10.5×10^6 lb per sq in., and $\alpha = \frac{E\,I}{h}\left(\frac{\Delta}{h}\right) = 156.5\,\Delta$.

The fixed-end moments are distributed, and the moments and the shear forces are shown in Fig. 10. The Q-forces and the P-loads are indicated in Fig. 11.

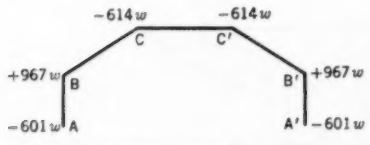

FIG. 9.—STRESSES AFTER DISTRIBUTION

Step 3.—In computing the longitudinal edge (plate) stresses at the middle section (in terms of Δ) corresponding to the P-loads in step 2, the relative deflection Δ, between the edges B and C, is assumed to vary as a sine curve, and hence the corresponding P-loads, bending moments, and stresses will vary as a sine curve.

Table 3 shows the computations for the bending moment at the middle of the span, and for the maximum fiber stresses. In these computations, the bending moment at midspan equals $P_0 \frac{L^2}{\pi^2}$, in which P_0 is the intensity of the load at the middle of the span.

TABLE 2.—DISTRIBUTION OF THE STRESSES PRODUCED BY EDGE FORCES, IN POUNDS PER SQUARE INCH[a]

Description	Edge A	Joint B		Joint C	
Distribution coefficients		0.58	0.42	0.5	0.5
Free edge stresses	−235	+235	+2105	−2105	0.0
Balance		+1085	−785	+1052	−1052
Carry over	−542		−526	+392	+526
Balance		−305	+221	+67	−67
Carry over	+152		−33	−110	+33
Balance		−19	+14	+72	−72
Carry over	+10		−36	−7	+36
Balance		−21	+15	+21.5	−21.5
Carry over	+10		−11	−7	+11
Balance		−6	+5	+9	−9
Carry over	+3		−4	−2	+4
Balance		−2	+2	+3	−3
Carry over	+1				
Distributed stresses	−601	+967	+967	−614	−614

[a] Multiply all stress values in this table by the unit load, w.

The free edge stresses shown in Fig. 12 are distributed by the stress distribution method to include the effect of the edge shears V. The same coefficients and method used in step 1 are used to solve for the stresses shown in Fig. 13.

Step 4.—In determining the displacements δ, parallel to the plate elements, the deflection at the middle of a beam loaded with a uniform load is given by

$$\delta_0 = \frac{s_0}{E\,h}\,\frac{5}{48}\,L^2 = \delta_1 \qquad (4)$$

to yield an approximate value of δ. The difference between the maximum fiber stresses at the middle of span L is expressed as s_0, and h is the depth of the beam.

The deflection[10] at the middle of a beam loaded with a distributed load varying as a half sine wave is expressed as

$$\delta_0 = \frac{s_0}{E\,h}\,\frac{L^2}{\pi^2} = \delta_2 \qquad (5)$$

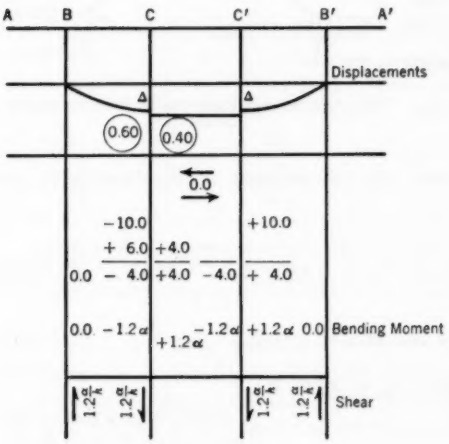

FIG. 10.—MOMENT AND SHEAR VALUES

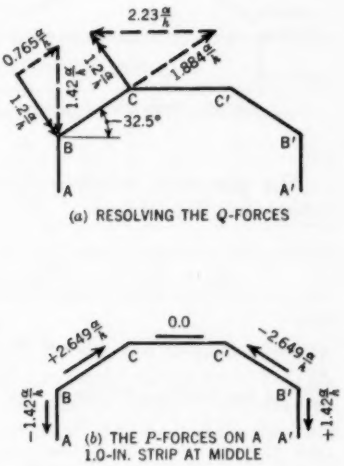

FIG. 11.—OBTAINING THE *P*-FORCES

TABLE 3.—COMPUTATIONS OF FREE EDGE STRESSES

Plate	Load intensity at midspan, P_0, in lb per in.	Bending moment at midspan, M_0, in in.-lb	Section modulus, Z, in in.^{3}	Maximum fiber stress, s_0, in lb per sq in.
(1)	(2)	(3)	(4)	(5)
AB	$-1.42\ \alpha/h$	$-50.40\ \alpha$	0.1354	$\pm 372.0\ \alpha$
BC	$+2.649\ \alpha/h$	$+94.10\ \alpha$	0.266	$\pm 353.0\ \alpha$
CC′	0.0	0.0	0.266	0.0

in which δ_2 is a correction to be applied to δ_1. Hence, the deflections δ of the plate elements produced by the two cases of loading discussed in steps 1 and 3 are as follows:

$$\delta_{ab} = \frac{(601 + 967)\,w}{E \times 2.50} \times \frac{5}{48} \times 35.0^2 - \frac{(329.7 + 287.3)\,\alpha}{E \times 2.50} \times \frac{35.0^2}{\pi^2}$$

[10] "The Analysis of Hipped Plate Structures Considering the Relative Displacements of the Joints," by Ibrahim Gaafar, thesis presented to the University of Michigan, at Ann Arbor, Mich., in 1949, in partial fulfilment of the requirements for the degree of Doctor of Science, Appendix II, pp. 107 to 111.

setting α equal to $156.5\,\Delta$ yields

$$\delta_{ab} = 7.63 \times 10^{-2}\, w - 0.457\,\Delta \quad \ldots\ldots\ldots\ldots\ldots\ldots (6a)$$

Similarly,

$$\delta_{bc} = -\,5.50 \times 10^{-3}\, w + 0.2195\,\Delta \quad \ldots\ldots\ldots\ldots\ldots\ldots (6b)$$

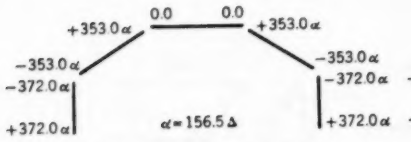

FIG. 12.—FREE EDGE STRESSES

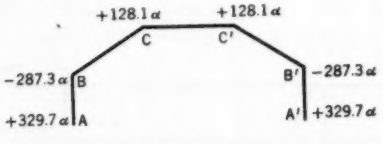

FIG. 13.—STRESSES PRODUCED BY DISPLACEMENTS OF JOINTS

The geometric relations between the components of displacements, as indicated in Fig. 14, are

$$\Delta_{bc} = \left(\delta_{bc} + \frac{\delta_{ab}}{\cos 57.5}\right) \cot 57.5 = 0.6371\,\delta_{bc} + 1.186\,\delta_{ab} \quad \ldots\ldots (7a)$$

and

$$\Delta_{cb} = \delta_{bc} \times \cot 32.5 = 1.57\,\delta_{bc} \quad \ldots\ldots\ldots\ldots\ldots\ldots (7b)$$

Adding Δ_{bc} and Δ_{cb} yields $\Delta = 2.2071\,\delta_{bc} + 1.186\,\delta_{ab}$.

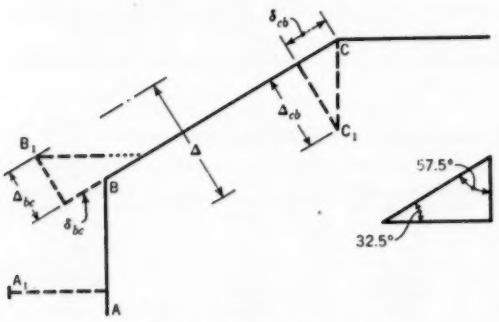

FIG. 14.—EDGE DISPLACEMENTS

Substituting the values given in Eqs. 6*a* and 6*b* for δ_{ab} and δ_{bc},

$$\Delta = 10.46 \times 10^{-3}\, w$$

in which Δ is expressed in inches.

Step 5.—Substitution of the value for Δ in the stress values obtained in step 3 yields stresses expressed in terms of the applied load w.

$$\alpha = 156.5\,\Delta = 1.638\, w$$

The maximum longitudinal stresses at the middle section of the model, as computed by the approximate theory,[2] together with those resulting from the relative displacements of joints and those computed by the proposed theory, are given in Table 4. The necessary correction for the relative displacement of the joints ranges in magnitude between 34% and 90% of the result of the approximate theory.

In computing the bending moment in a transverse strip 1.0 in. wide, the approximate theory, in which external loads and nonyielding supports are

considered, yields as the connecting moment $-M_c = 0.05\, w\, h^2 = 0.612\, w$. The maximum moment in span CC′ is $\frac{w\, h^2}{8} = 1.530\, w$. Both moments are in units of inches-pounds, and are illustrated by "Case 1" in Fig. 15. "Case 2" is the moment resulting from the relative deflection of joints, in inches-pounds:

TABLE 4.—THE MAXIMUM LONGITUDINAL STRESSES, IN POUNDS PER SQUARE INCH, PRODUCED BY A UNIFORM LOAD ON THE MODEL OF EXAMPLE No. 1[a]

Edge	Method of Computation		
	"Approximate" theory	Joint displacement	Proposed theory[b]
(1)	(2)	(3)	(4)
C	−614	+210	−404
B	+967	−470	+497
A	−601	+540	−61

[a] Multiply all stress values in this table by the unit load, w. [b] To obtain the values in Col. 4, add the values in Col. 2 to those in Col. 3.

$M_c = 1.2\, \alpha = 1.20 \times 1.638\, w = 1.96\, w$. In "Case 3," the proposed theory, the moments are added, as shown by the bending moment diagrams in Fig. 15.

A serious change in the transverse bending moment of "Case 1" is caused by the relative displacements of the joints, the increase in the value of the bending moment being $\frac{1.96}{0.918} \times 100 = 213\%$ at the middle of span CC′, and $\frac{-1.96}{0.612} \times 100 = -320\%$ at joints C and C′.

TABLE 5.—COMPUTATION OF PLATE LOADS, MOMENTS, AND STRESSES[a]

Plate	Load, P, in pounds	Free edge bending moment, M_e, in inch-pounds	Maximum fiber stress, s_e, in pounds per square inch
(1)	(2)	(3)	(4)
AB	0.0	0.0	0.0
BC	−0.466	−5.24	±20.45
CC′	0.0	0.0	0.0

[a] Multiply all values in this table by the total load, W.

Example No. 2.—The same aluminium model of Example No. 1 will be analyzed for the case of four concentrated vertical forces of 58.35 lb. each, acting on the model as shown in Fig. 16. The maximum longitudinal and the maximum transverse stresses at the middle of the model will be computed, and will subsequently be compared with the experimental results obtained for the same case.

Step 1.—For the case of external loads acting at the joints, the loads $W/4$ are resolved in the directions of the two adjacent plates (assuming nonyielding supports). The P-loads acting on the plates (Fig. 17) are yielded directly. These loads, and the resulting moments and stresses at the middle section, are listed in Table 5. The free edge stresses are shown in Fig. 18. Using the same stress distribution procedure and the same coefficients given in the preceding example, the stresses after distribution are as shown in Fig. 19.

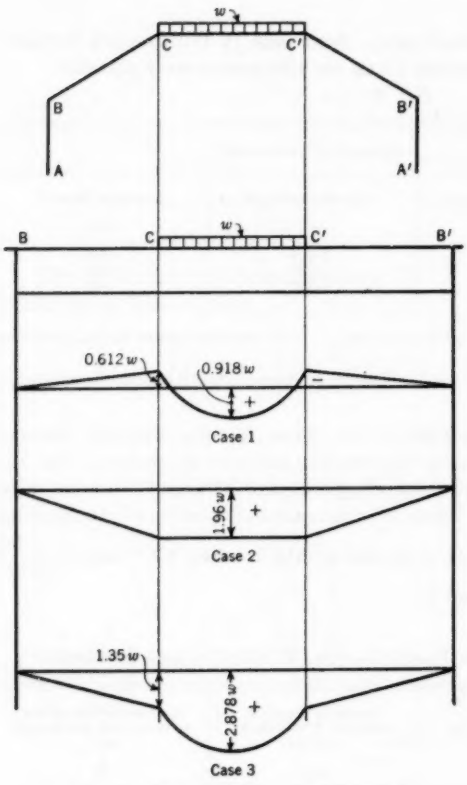

FIG. 15.—TRANSVERSE BENDING MOMENTS

Steps 2 and 3.—The procedure and the results for these steps are identical with those in Example No. 1.

Step 4.—The deflection[9] at the middle of a beam loaded with two concentrated loads at the $\frac{1}{3}$-points of the span is $\delta_0 = \frac{s_0 L^2}{E h} \times \frac{23}{216} = \delta_1$, in which s_0 is the difference between the maximum fiber stresses at the middle of span L.

The deflection[10] at the middle of a beam loaded with a distributed load varying as a half sine wave is expressed by $\delta_0 = \frac{s_0}{E h} \times \frac{L^2}{\pi^2} = \delta_2$. Hence, the deflections δ of the plate elements due to the two cases of loading, described in steps 1 and 3, are as follows:

$$\delta_{ab} = \frac{(4.26 + 8.53)}{E \times 2.50} \times W \times 35.0^2 \times \frac{23}{216} - 0.457\,\Delta$$

$$= + \frac{670}{E} W - 0.457\,\Delta$$

$$= 0.638 \times 10^{-4} W - 0.457\,\Delta.$$

Similarly,

$$\delta_{bc} = - 0.510 \times 10^{-4} W + 0.2195\,\Delta.$$

The geometrical relations between the components of the edge displacements of the model hold true and are independent of the applied loads. The same geometrical relation of Example No. 1 will be used herein, namely: $\Delta = 2.2071\ \delta_{bc} + 1.186\ \delta_{ab}$. Substituting the values given for δ_{ab} and δ_{bc} into the geometrical relation yields $\Delta = 0.928 \times 10^{-4}\ W$ in. The positive sign of Δ indicates that Δ is assumed in the correct direction.

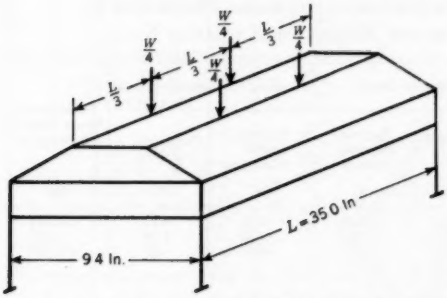

FIG. 16.—APPLICATION OF LOADS, EXAMPLE NO. 2

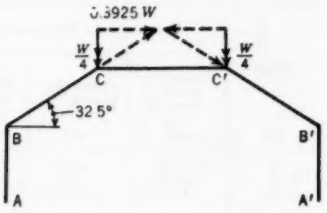

FIG. 17.—DETERMINATION OF *P*-LOADS

Step 5.—Substituting the value for Δ in the stresses obtained in step 3 gives these stresses expressed in terms of the applied load, W:

$$\alpha = E\,\Delta\,(14.90) \times 10^{-6} = 156.5\,\Delta$$
$$= 156.5 \times 0.928 \times 10^{-4}\,W = 0.0145\,W.$$

The applied load is $W = 4 \times 58.35 = 233.4$ lb.

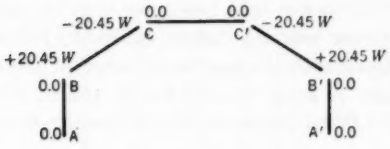

FIG. 18.—FREE EDGE STRESSES

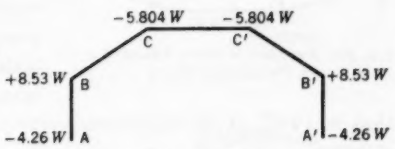

FIG. 19.—STRESSES AFTER DISTRIBUTION

The maximum longitudinal stresses at the middle section of the model, obtained by means of the approximate theory,[2] the relative displacements of the joints and the proposed theory are listed in Table 6, together with the experimental results. The methods of analysis are found in the column headings, of Table 6.

The necessary correction ranged between 32% and 112% of the approximate values, and resulted in changing the sign of the stress at edge A.

The bending moment diagram on a transverse strip 1.0 in. wide, at the middle of the model, is shown in Fig. 20. No transverse bending moment is found by the approximate theory because the external loads are applied directly at the joints. Consideration of the relative displacements of the joints yields

$M_e = 1.2\,\alpha = 1.2 \times 0.0145\,W = 4.065$ in.-lb. Superposition of these two conditions yields the result by the proposed theory.

The maximum fiber stresses corresponding to this bending moment are

$$s = \pm \frac{M\,y}{I} = \pm \frac{4.065}{183 \times 10^{-6}} \times \frac{0.13}{2} = \pm 1{,}440 \text{ lb per sq in.}$$

TABLE 6.—MAXIMUM LONGITUDINAL STRESSES PRODUCED BY CONCENTRATED LOADS ON THE MODEL OF EXAMPLE NO. 2

Edge	Stresses, in Pounds per Square Inch				Error, in Percentages		Stresses by beam theory (lb per sq in.)
	"Approximate" theory	Joint displacement	Proposed theory[a]	Experimental values	"Approximate" theory	Proposed theory	
(1)	(2)	(3)	(4)	(5)	(6)	(7)	(8)
C	−1,360	+435	−925	−820	+66	+13	−537
B	+2,000	−980	+1,020	+740	+170	+38	+166
A	−1,000	+1,122	+122	+378	−365	−68	+1,102

[a] Values in Col. 4 are found by adding the values in Col. 2 to those in Col. 3.

The tensile force in plate CC′ found by relative displacements of the joints is $P_{cc'} = 2.23\,\frac{\alpha}{h} = 2.23 \times \frac{0.0145\,W}{3.5} = 0.00924\,W = 2.16$ lb per longitudinal in. The corresponding direct stress is + 16.6 lb per sq in., in tension.

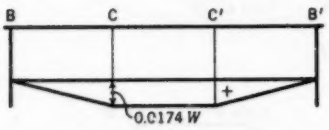

FIG. 20.—BENDING MOMENT DIAGRAM FOR A TRANSVERSE STRIP

In the foregoing example, it should be noted that, although the approximate theory does not take into consideration any transverse bending stresses caused by joints displacements, the maximum value for these stresses is equal to ± 1,440 lb per sq in., that is, 141% of the maximum value of 1,020 lb per sq in. for the longitudinal stresses.

EXPERIMENTAL INVESTIGATION

Description of the Model.—An aluminium (24 S-T) model on a $\frac{1}{40}$-scale was used for the experimental investigation of the distribution of stresses and strains in a hipped plate structure. The general dimensions of the model are shown in Fig. 21. The supporting angles and base plates were of steel. The load was applied at four points on the model, as shown by the arrows on the diagrams in Fig. 21. To measure the longitudinal strains, SR-4 resistance gages (types A1 and A12) were placed at section C-C, D-D, and E-E. These longitudinal gages were placed on both sides of the plate and connected in series to yield the average strain. Transverse strains were measured at eight points by means of type A7 resistance gages. These gages are represented by

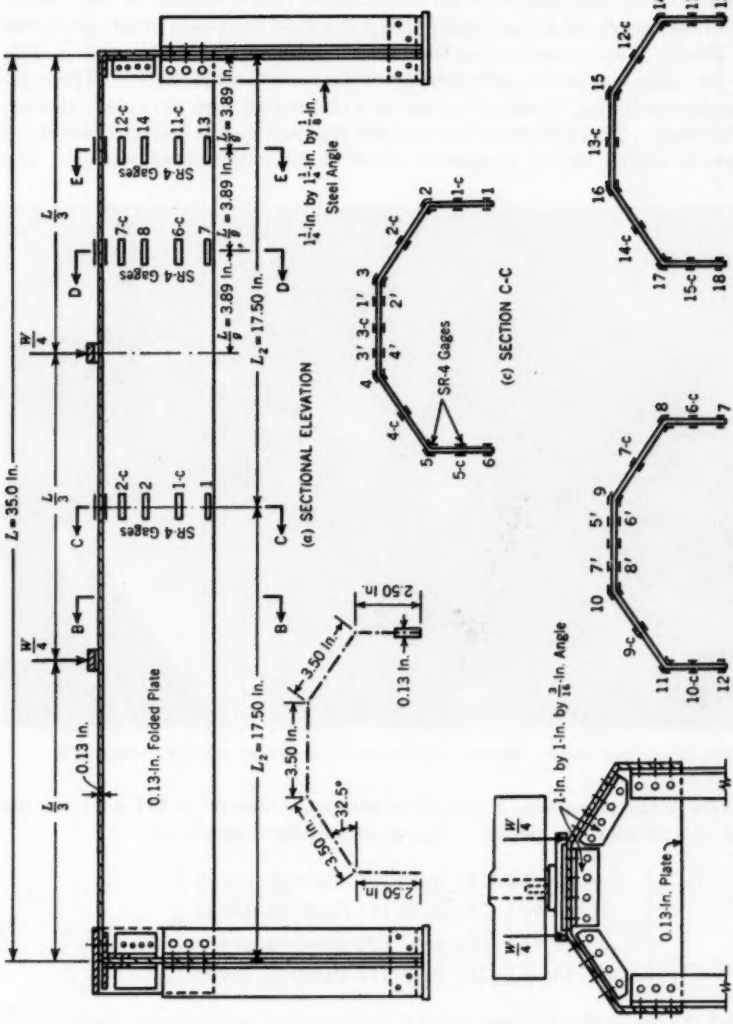

FIG. 21.—DETAILS OF THE HIPPED PLATE ROOF MODEL

1′, 2′, 3′, ⋯, 8′ as indicated in Figs. 21(*c*) and 21(*d*). These gages (on both sides of a plate element) were wired independently, thus giving the transverse strains at the outer and inner surfaces of the roof separately. A picture of the model appears as Fig. 22.

Results.—The distribution of the longitudinal (plate) strains at the middle section of the model, for a total load of 233.4 lb (58.35 lb at each point), is shown in Fig. 23(*a*). The corresponding transverse (slab) strains − 82, − 96, + 140, and + 143 micro-in. per in. are recorded in the circles in Fig. 23(*b*). The compressive strains in Fig. 23 are indicated by a minus sign, and the tensile strains, by a plus sign. The difference between the readings on the top and bottom of the plate is caused by the transverse effect of the longitudinal strains. The

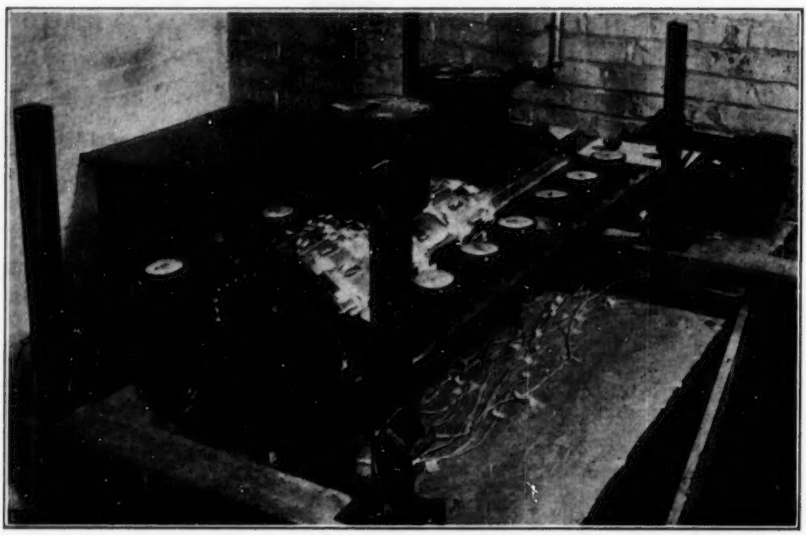

FIG. 22.—LOADED MODEL, SHOWING DIAL GAGES, STRAIN GAGES, AND STRAIN INDICATOR

true value of the transverse strain is the average strain, or ± 111 micro-in. per in. and ± 119 micro-in. per in. This checks quite closely with

$$\left.\begin{aligned} -82 - \tfrac{1}{3}(78) &= -108 \text{ micro-in. per in.} \\ +140 - \tfrac{1}{3}(78) &= +114 \text{ micro-in. per in.} \\ -96 - \tfrac{1}{3}(78) &= -122 \text{ micro-in. per in.} \\ +143 - \tfrac{1}{3}(78) &= +117 \text{ micro-in. per in.} \end{aligned}\right\} \quad \cdots\cdots\cdots\cdots (8)$$

in which $\frac{1}{3}(78)$ is the Poisson ratio ($\frac{1}{3}$), times the longitudinal strain (− 78 micro-in.).

The longitudinal strains at sections D-D and E-E in Figs. 21(*d*) and 21(*e*) are shown in Figs. 24(*a*) and 24(*b*). The average values of the strain for both sides of the structure are also shown. These diagrams show that the behavior

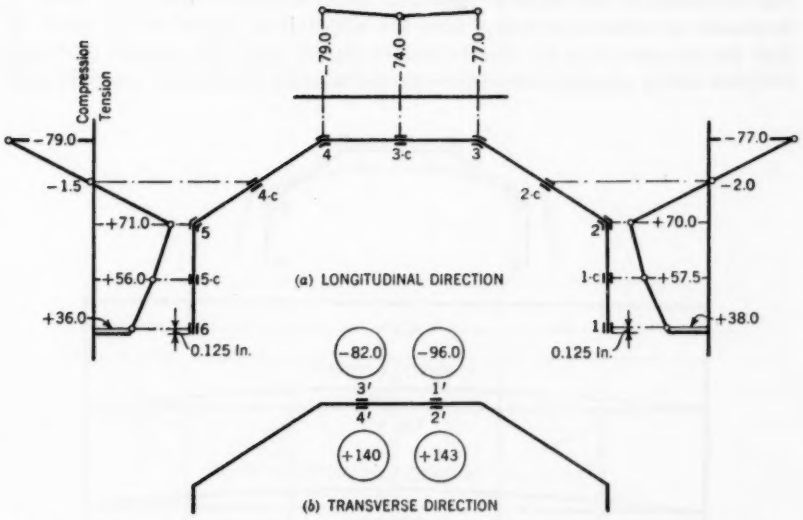

FIG. 23.—DISTRIBUTION OF UNIT STRAINS AT MIDDLE SECTION OF MODEL, IN MICRO-INCHES PER INCH

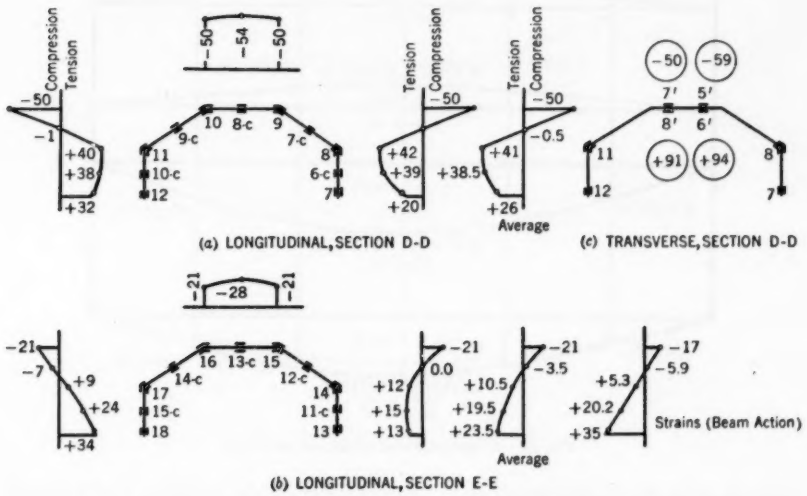

FIG. 24.—STRAINS AT CERTAIN SECTIONS OF THE MODEL, IN MICRO-INCHES PER INCH

at section D-D is similar to that at the middle, section C-C. This fact indicates that the effect of the relative transverse displacements of the joints seems to dominate the structural action over the middle two thirds of the span. It may also be noted that the longitudinal strains for these two sections (D-D and C-C) are nearly proportional to the external bending moments at these sections,

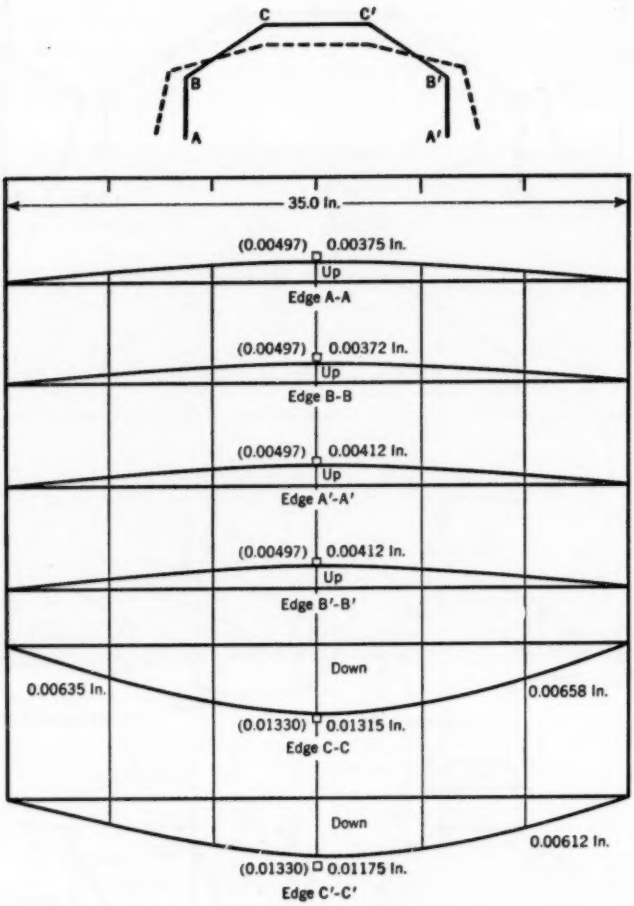

FIG. 25.—VERTICAL DISPLACEMENTS OF EDGES

computed on the basis of simple end supports. However, at section E-E, where the translation of the edges is small, the distribution of the longitudinal strains more nearly approaches that for ordinary beam action, as shown, although some effect of the change of shape of the cross section is apparent. Transverse strains at section D-D are shown in Fig. 24(*c*).

The measured vertical and horizontal displacements of the edges are shown in Figs. 25 and 26, respectively. The theoretical displacements (in inches) computed according to the proposed theory are shown between parentheses in the same figures. The vertical displacements of the elements AB and A′B′ are upward, which agree with the theoretical value obtained. This motion is

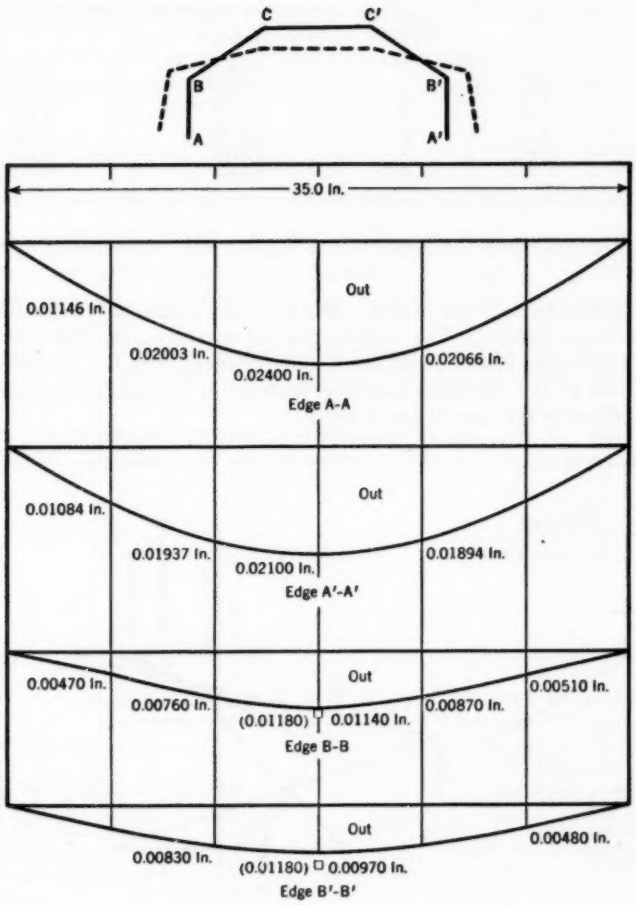

FIG. 26.—HORIZONTAL DISPLACEMENTS OF EDGES

comparatively small, but very significant. The horizontal movements of edges B and B′ are of the same order of magnitude as the vertical movements of C and C′. A comparison of the theoretical and measured values of edge translations is given in Table 7. The computed values of the displacements agreed quite well with the measured values.

The longitudinal stresses determined by the different theories and test results are listed in Table 6 and are presented graphically in Fig. 27. The correction diagram corresponding to edge translation is included in Fig. 27. The

TABLE 7.—Model Deflections at the Middle Section (Example No. 2)

Edge	Plate	Types of deflections	Deflections computed by the proposed theory, in inches	Deflections evaluated experimentally, in inches
A′	A′B′	δ	0.00497	0.00412
B′	B′A′	δ	0.00497	0.00412
B′	B′A′	Δ	0.0118	0.0097
B	BA	Δ	0.0118	0.0114
B′	B′C′	Δ	0.0105	0.0092
C′	C′B′	Δ	0.0112	0.0099
C	CB	Δ	0.0112	0.0111
C	CC′	Δ	0.0133	0.0131

experimental values of the longitudinal stresses clearly indicate the following facts:

1. The structure, under loading, does not behave as a unit according to the ordinary beam theory. The distribution of measured longitudinal stresses (Fig. 27) is nearly linear across each plate element, but the stresses are not proportional to the distances from the centroid of the entire cross section, as they would be in the case of beam action.

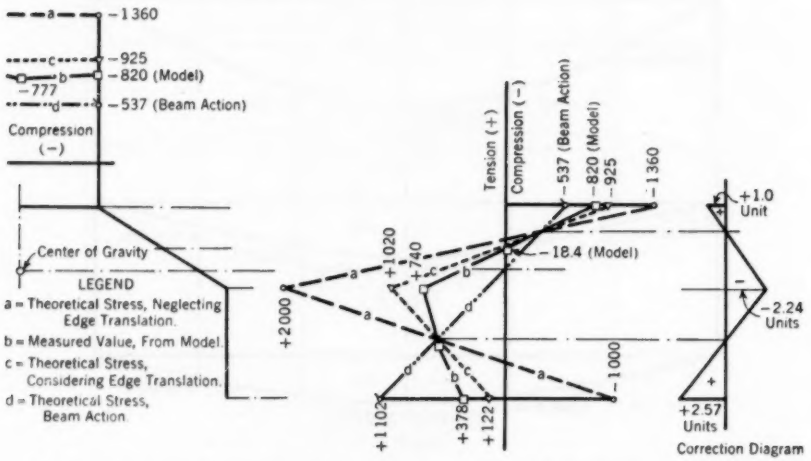

Fig. 27.—Comparison Between the Measured and Theoretical Longitudinal Stresses at the Middle Section of the Model, in Pounds per Square Inch

2. When the relative transverse displacements of the joints are not taken into consideration, the stress values as computed by the approximate theory are much higher than the experimental values. The errors at the joints from top to bottom of the cross section (Fig. 27) are (joint C) + 66%, (joint B) + 170%, and (joint A) − 365%. These errors are given in Table 6.

3. The approximate theory may not even predict the right sense of the longitudinal stresses, as shown by the opposite signs obtained at edges A and A′ for experimental and current theoretical values.

4. On the other hand, when the relative displacements of the joints are considered, the values of the longitudinal stresses agree much better with

TABLE 8.—MAXIMUM TRANSVERSE STRESSES, IN POUNDS PER SQUARE INCH (EXAMPLE NO. 2)

Points (see Fig. 28)	Values obtained experimentally	Values yielded by the proposed theory	Average percentage of error
(1)	(2)	(3)	(4)
1′ and 2′	∓1,170	∓1,440	18.5
3′ and 4′	∓1,260	∓1,440	

the experimental results. The errors at the joints from top to bottom of the cross section are (joint C) 13%, (joint B) 38%, and (joint A) − 68%, respectively—that is, about one fifth of the corresponding errors produced by the approximate theory.

The transverse stresses determined experimentally and by the proposed theory are listed in Table 8 and are presented graphically in Fig. 28, in which the measured values of stresses are indicated by small circles. These stresses correspond to the transverse strains shown in Figs. 23 and 24. Because the relative joints displacements are neglected in the approximate theory, the

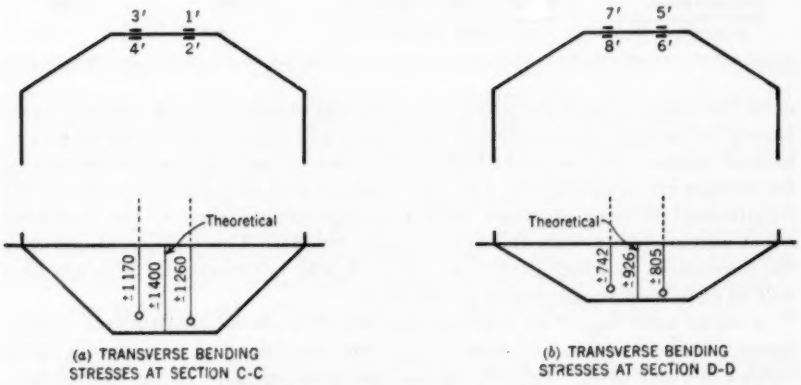

FIG. 28.—COMPARISON BETWEEN THEORETICAL AND EXPERIMENTAL TRANSVERSE STRESSES IN THE MODEL (ALL STRESSES IN POUNDS PER SQUARE INCH)

values of the transverse stresses yielded thereby are zero. From the results presented in Table 8 and in Fig. 28, together with the comments at the end of Example No. 1 and Example No. 2, it can be noted that:

a. Although the transverse stresses are of the same order of magnitude as the longitudinal stresses (or even larger), the approximate theory misses them

completely in the case of concentrated loads acting at the joints, or of tangential forces acting on the plates.

b. In the case of uniform loads acting on the roof (Example No. 1), the approximate theory still errs greatly on the unsafe side, the error being in the neighborhood of from + 60% to − 280%. The error in the transverse bending moment (Fig. 15) that governs the slab design is quite serious.

c. The proposed theory presents a correct picture of the transverse stresses in the cases of concentrated, tangential, or uniform loads.

d. The error in the case of the proposed theory is on the safe side and is in the neighborhood of only 19%, as is indicated in Fig. 28.

The correction diagram representing the effect of joints displacements on the longitudinal stresses is shown separately in Fig. 27. An interesting fact brought out in Fig. 27 is that the different longitudinal stress diagrams pass through two common points which correspond to the two zero points of the correction diagram. This condition indicates that, if the ordinates of the correction diagram are multiplied by a proper constant and subtracted algebrai-

TABLE 9.—CHECK ON THE EXPERIMENTAL AND LONGITUDINAL STRESSES AT THE MIDDLE SECTION OF THE MODEL

Determination of stresses	Summation of stresses, in pounds per square inch	Bending Moments, in Inch-Pounds	
		Internal	External
Experimental	$E \Sigma \epsilon\, dA = E(-69.75 + 69.449) \approx 0.0$	+ 1,357	+ 1,350
Proposed theory	$\Sigma s\, dA = -842 + 837 \approx 0.0$	+ 1,357	+ 1,360
Joints displacement (Correction diagram)	$\Sigma s\, dA = -0.564 + 0.564 = 0.0$	0.0	0.0

cally from the values of the longitudinal stresses obtained by the ordinary beam theory for the entire cross section, the results will agree closely with the experimental values. On the other hand, if the longitudinal stresses accompanying translation are multiplied by a proper constant and added algebraically to the longitudinal stresses obtained from the approximate theory, the combined effect agrees closely with the experimental results. These observations raise the question as to which analytical approach may be desirable. This question will be examined subsequently in the paper.

Checks were made[11] of experimental and theoretical longitudinal stresses against basic equations of equilibrium, the conditions of equilibrium being fulfiled in every case. Table 9 summarizes these results. In the equations in Table 9, ϵ represents the unit linear strains, and A the cross-sectional area of the metal.

Hipped Plate Structures Compared with Ordinary Beams.—In hipped plate structures, the thickness *t* of each plate element is relatively small as compared to the other dimensions of the cross section of the structure. Consequently,

[11] "The Analysis of Hipped Plate Structures Considering the Relative Displacements of the Joints," by Ibrahim Gaafar, thesis presented to the University of Michigan at Ann Arbor, Mich., in 1949, in partial fulfilment of the requirements for the degree of Doctor of Science, Appendix III, pp. 112–117.

the section of the structure changes its shape under loading, and the part of the load carried by each plate element varies with the position of the load on the cross section (Fig. 29), depending on the position of the load relative to the plate element under consideration. Also, there are forces and bending moments acting in the transverse direction (slab action). The condition of a plane section before deformation remaining plane after deformation does not hold for the cross section as a whole, except under very special cases of loading; but it holds fairly well for each individual plate element, especially for cross sections that are distant from the diaphragm.

If a member under load is to behave as an ordinary beam, certain requirements must be fulfiled. The thickness t should be large enough in comparison with the other dimensions of the cross section to prevent the section from changing its shape when the member is deflected longituidnally under loading—otherwise, internal diaphragms must be used to prevent distortion of the cross section. Under ordinary beam action, the cross section only moves parallel to itself, and the whole cross-sectional plane that existed before bending remains plane after bending. No transverse bending or deflection should exist under beam action, or the section will change its shape. Referring to Fig. 29, the longitudinal stress distribution over the cross section is not affected by changing the points of application of the loads, so long as the loads are symmetrical with

FIG. 29.—SYMMETRICAL LOADING

respect to the vertical axis of symmetry of the cross section. Each plate element of the member carries a constant fraction of the total applied load, depending only on the dimensions of the cross section. Beam action can be a very special case in the behavior of a hipped plate structure under the following conditions: External forces must be either line loads or concentrated loads acting only at the edges and distributed in a very special manner so that each of the final resultant P-loads on each individual plate equals the P-load on the same plate if the structure were to behave as an ordinary beam. Any distributed load or concentrated load acting in between the joints will result in transverse bending and, consequently, in a change in the shape of the cross section.

Therefore, it is evident that, if an effort is made to solve the hipped plate roof described previously by beginning from the preliminary assumption of a beam action and trying to correct it to obtain the longitudinal stresses of a hipped plate structure, two corrections for the longitudinal stresses obtained from beam action must be applied. These corrections are as follows:

(*a*) Longitudinal stresses resulting from the difference between the plate loads P included in the assumption of beam action, and the plate loads P obtained from the actual external loads, must be included. Under the pre-

liminary assumption of beam action, a certain part of the total loads must be assumed to be carried by each plate element, which is not necessarily the case. However, beam action can be acquired by applying certain restraining line loads along the joints, and removing them by means of the first correction. The analytical work for carrying out this correction is very similar to that used in correcting for the relative displacements of the joints.

(*b*) Longitudinal stresses corresponding to the change in the *P*-loads resulting from the relative deflections of the joints must be determined because, in beam action, transverse deflections are not taken into consideration. The writer has described the procedure for this correction previously.

It can be seen from the foregoing discourse that more analytical work will be involved by trying to solve the problem from the beam action approach because correction for the relative displacements of the joints must be made.

Summary and Conclusions

A (24 S-T) aluminium model is both convenient and satisfactory for studying the structural action of hipped plate roofs. The effect of the relative displacements of the joints appears to dominate the structural action over the middle two thirds of the span. If the relative displacements of the joints are eliminated by introducing more intermediate diaphragms, the longitudinal stresses of a hipped plate roof will approach those of an ordinary beam. An analysis by the approximate theory or by beam action is erroneous unless corrected for the effect of relative joint displacements.

The longitudinal stresses obtained from the approximate theory are much higher than the measured values, the average discrepancy being about 200% for the approximate theory, and 40% for the proposed theory. At certain edges (A and A′), the sign of the longitudinal stresses predicted by the proposed treatment is confirmed, and that predicted by the current theory is opposed by the experimental results. The transverse stresses, fundamental for the design of the plates as a continuous slab, are even more seriously affected by joints displacements. The approximate theory errs greatly on the unsafe side. The necessary correction to be applied to the transverse stresses found by that theory may be as much as 320%, with a change of sign (see Example No. 1). In the case of concentrated loads at the joints (Example No. 2), the maximum transverse stresses were experimentally found to be 150% of the maximum longitudinal stresses. The proposed treatment gives a correct picture of the experimental stresses both in magnitude and in sign, the discrepancy being 20% on the safe side.

The proposed theory offers a solution for the problem in the form of simple linear algebraic equations in which the number of unknowns is $(r - 1)$ for unsymmetrical loading and $\binom{r}{2} - 1$ for symmetrical loading, in which r is the number of joints. For a roof of five plates (that is, four joints) the number of equations is three for unsymmetrical loading and one for symmetrical loading.

Further Investigation

The effect of intermediate diaphragms and the effects of change of thickness t, width h, and span L of plate elements, on the behavior of the model, all merit investigation. The effect of the shape of the cross section on the behavior of the model is worthy of study, and the effect of continuous spans in both directions should be considered. Deep beam action is a subject affecting this type of structure. Studies of the behavior of models just before failure and of reinforced concrete models are also suggested.

Acknowledgments

The writer wishes to express his appreciation to L. C. Maugh, M. ASCE, of the University of Michigan, at Ann Arbor, for his valuable advice and suggestions in regard to the conduct of this work, and for the time he has kindly given for consultation.

The writer wishes to thank the ASCE reviewers for criticism, the meeting of which added considerably to the clarity of the paper. Thanks are also due to the Egyptian Education Bureau at Washington, D. C., and to the Engineering Research Institute of the University of Michigan for partly financing the work.

APPENDIX. NOTATION

The following symbols, adopted for use in the paper, and for the guidance of discussers, conform essentially with American Standard Letter Symbols for Structural Analysis (ASA—Z10.8—1942), prepared by a Committee of the American Standards Association, with Society representation, and approved by the Association in 1942:

A = the cross-sectional area of a plate, $h\,t$;

a, b, c = the subscripts used to denote edges and plate elements A, B, $\cdots$, etc.;

c = the stiffness coefficient of a member;

h_{ab} = the width of plate AB, or distance between edges A and B measured along the center line of the cross section of a plate;

k = the rigidity coefficient $\left(k = \frac{E\,I}{h} \right)$;

L = the span of the roof between end diaphragms;

P = the force components of the slab shears Q, parallel to the adjacent plates and resisted by plate action;

Q_{bc} = the slab shearing force per unit length, acting from joint B on plate BC in the direction perpendicular to BC;

t_{ab} = the thickness of plate AB;

V_b = the shear stresses per unit length parallel to edge B, acting from joint B along the edges of the adjacent plates;

Z = the section modulus of a plate, considered to act as a beam $\left(Z = \frac{t\,h^2}{6}\right)$;

0 = the subscript used to denote the middle of a beam or a plate;

Δ_{bc} = the component of the displacement of edge B perpendicular to plate BC, corresponding to slab action;

Δ_{cb} = the component of the displacement of edge C perpendicular to plate BC (slab action);

δ_{bc} = the component of the displacement of edge B in the plane of plate BC (plate action);

$\delta_{cb} = \delta_{bc}$;

δ_0 = the deflection at the middle of a beam;

δ_1 = the plate deflection at its middle according to the approximate theory; and

δ_2 = the correction to the plate deflection produced at the middle section by the relative transverse displacements of the joints.

CURRENT PAPERS

Proceedings-Separate Number	Title and Author	Discussion closes*
159	"Development of a Flood-Control Plan for Houston, Tex.," by Ellsworth I. Davis	June 1
160	"Ice Pressure Against Dams: Studies of the Effects of Temperature Variations," by Bertil Löfquist	June 1
161	"Ice Pressure Against Dams: Some Investigations in Canada," by A. D. Hogg	June 1
162	"Ice Pressure Against Dams: Experimental Investigations by the Bureau of Reclamation," by G. E. Monfore	June 1
163	"A Comparison of Design Methods for Airfield Pavements," Progress Report of the Committee on Correlation of Runway Design Procedures of the Air Transport Division	June 1
164	"Water Supply Engineering," Report of Committee on Water Supply Engineering of the Sanitary Engineering Division for the Period Ending September 30, 1951	July 1
165	"Design Curves for Anchored Steel Sheet Piling," by Walter C. Boyer and Henry M. Lummis, III	July 1
166	"The Design of Flexible Bulkheads," by James R. Ayers and R. C. Stokes	July 1
167	"Sewage Disposal in Tidal Estuaries," by Alexander N. Diachishin, Seth G. Hess, and William T. Ingram	July 1
168	"Special Design Features of the Yorktown Bridge," Maurice N. Quade	July 1
169	"Rating Curves for Flow over Drum Gates," by Joseph N. Bradley	Aug. 1
170	"Rapid Computation of Flexural Constants," by Thomas G. Morrison	Aug. 1
171	"Unified Mass-Transportation System for New York," by William Reid	Aug. 1
172	"Aeronautical Charting and Mapping," by Charles A. Schanck	Aug. 1
173	"Electronic Devices for Air Transport," by F. B. Lee	Aug. 1
174	"Zoning Maps for Airports," by Benjamin Everett Beavin, Sr.	Aug. 1
175	"Design of Side Walls in Chutes and Spillways," by D. B. Gumensky	Aug. 1
176	"Advances in Sewage Treatment and Present Status of the Art," Progress Report of the Committee of the Sanitary Engineering Division on Sewerage and Sewage Treatment	Sept. 1
177	"Earthquake Stresses in Shear Buildings," by M. G. Salvadori	Sept. 1
178	"Rainfall Studies Using Rain-Gage Networks and Radar," by H. E. Hudson, Jr., G. E. Stout, and F. A. Huff	Sept. 1
179	"Stiffness Charts for Gusseted Members Under Axial Load," by John E. Goldberg	Sept. 1
180	"A Direct Step Method for Computing Water-Surface Profiles," by Arthur A. Ezra	Sept. 1
181	"Slackwater Improvement of the Columbia River," by O. E. Walsh	Oct. 1
182	"Hipped Plate Analysis, Considering Joint Displacement," by Ibrahim Gaafar	Oct. 1
183	"Group Loadings Applied to the Analysis of Frames, by I. F. Morrison	Oct. 1
184	"Dam Modifications Checked by Hydraulic Models," by E. S. Harrison and Carl E. Kindsvater	Oct. 1
185	"Nonelastic Behavior of Bridges Under Impulsive Loads," by S. J. Fraenkel and L. E. Grinter	Oct. 1
186	"Settling Rates of Suspensions in Solids Contact Units," by A. A. Kalinske	Oct. 1
187	"The Equivalent Rectangle in Prestressed Concrete Design," by John J. Peebles	Oct. 1
188	"Laminar to Turbulent Flow in a Wide Open Channel," by W. M. Owen	Oct. 1

* Readers are urged to submit discussion applying to current papers. Forty free Separates per year are allotted to members. Mail the coupon order form found in the current issue of *Civil Engineering*.

AMERICAN SOCIETY OF CIVIL ENGINEERS

OFFICERS FOR 1953

PRESIDENT

WALTER LEROY HUBER

VICE-PRESIDENTS

Term expires October, 1953:

GEORGE W. BURPEE
A. M. RAWN

Term expires October, 1954:

EDMUND FRIEDMAN
G. BROOKS EARNEST

DIRECTORS

Term expires October, 1953:

KIRBY SMITH
FRANCIS S. FRIEL
WALLACE L. CHADWICK
NORMAN R. MOORE
BURTON G. DWYRE
LOUIS R. HOWSON

Term expires October, 1954:

WALTER D. BINGER
FRANK A. MARSTON
GEORGE W. McALPIN
JAMES A. HIGGS
I. C. STEELE
WARREN W. PARKS

Term expires October, 1955:

CHARLES B. MOLINEAUX
MERCEL J. SHELTON
A. A. K. BOOTH
CARL G. PAULSEN
LLOYD D. KNAPP
GLENN W. HOLCOMB
FRANCIS M. DAWSON

PAST-PRESIDENTS

Members of the Board

GAIL A. HATHAWAY
CARLTON S. PROCTOR

TREASURER

CHARLES E. TROUT

EXECUTIVE SECRETARY

WILLIAM N. CAREY

ASSISTANT TREASURER

GEORGE W. BURPEE

ASSISTANT SECRETARY

E. L. CHANDLER

PROCEEDINGS OF THE SOCIETY

HAROLD T. LARSEN
Manager of Technical Publications

DEFOREST A. MATTESON, JR.
Assoc. Editor of Technical Publications

PAUL A. PARISI
Asst. Editor of Technical Publications

COMMITTEE ON PUBLICATIONS

LOUIS R. HOWSON

FRANCIS S. FRIEL
I. C. STEELE
GLENN W. HOLCOMB
FRANK A. MARSTON
NORMAN R. MOORE